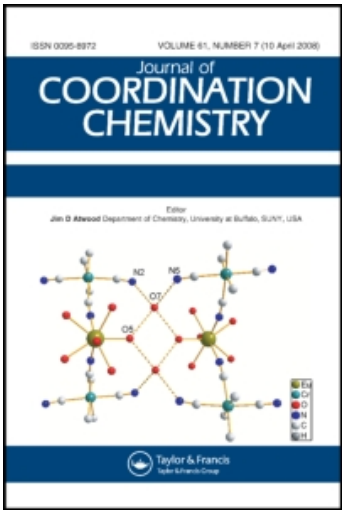

Journal of Coordination Chemistry
Publication details, including instructions for authors and subscription information:
http://www.informaworld.com/smpp/title~content=t713455674

Synthesis, characterization, photocleavage, antimicrobial activity and DNA binding of $[Co(bpy)_2MHPIP]^{3+}$, $[Co(dmb)_2MHPIP]^{3+}$, and $[Co(phen)_2MHPIP]^{3+}$ complexes

Kotha Laxma Reddy[a]; K. Ashwini Kumar[a]; S. Vidhisha[a]; P. Naga Babu[a]; S. Satyanarayana[a]
[a] Department of Chemistry, Osmania University, Hyderabad 500007, India

First published on: 22 September 2010

To cite this Article Reddy, Kotha Laxma , Kumar, K. Ashwini , Vidhisha, S. , Babu, P. Naga and Satyanarayana, S.(2009) 'Synthesis, characterization, photocleavage, antimicrobial activity and DNA binding of $[Co(bpy)_2MHPIP]^{3+}$, $[Co(dmb)_2MHPIP]^{3+}$, and $[Co(phen)_2MHPIP]^{3+}$ complexes', Journal of Coordination Chemistry, 62: 24, 3997 — 4008, First published on: 22 September 2010 (iFirst)
To link to this Article: DOI: 10.1080/00958970903215081
URL: http://dx.doi.org/10.1080/00958970903215081

Journal of Coordination Chemistry
Vol. 62, No. 24, 20 December 2009, 3997–4008

Taylor & Francis
Taylor & Francis Group

Synthesis, characterization, photocleavage, antimicrobial activity and DNA binding of $[Co(bpy)_2MHPIP]^{3+}$, $[Co(dmb)_2MHPIP]^{3+}$, and $[Co(phen)_2MHPIP]^{3+}$ complexes

KOTHA LAXMA REDDY, K. ASHWINI KUMAR, S. VIDHISHA, P. NAGA BABU and S. SATYANARAYANA*

Department of Chemistry, Osmania University, Hyderabad 500007, India

(*Received 21 June 2008; in final form 2 July 2009*)

4-Methyl-2-(2-hydroxyphenyl)imidazo[4,5-f][1,10]phenanthroline) (MHPIP) and its complexes $[Co(bpy)_2MHPIP]^{3+}$ (**1**) (bpy = 2,2′-bipyridine), $[Co(dmb)_2MHPIP]^{3+}$ (**2**) (dmb = 4,4′-dimethyl-2,2′-bipyridine), and $[Co(phen)_2MHPIP]^{3+}$ (**3**) (phen = 1,10-phenanthroline) have been synthesized and characterized by UV/VIS, IR, EA, ^1H, ^{13}C-NMR, and mass spectra. The binding of the three complexes with calf-thymus-DNA (CT-DNA) has been investigated by absorption and emission spectroscopy, DNA-melting techniques, viscosity measurements, and DNA cleavage assay. The spectroscopic data and viscosity results indicate that these complexes bind to CT-DNA via an intercalative mode. The complexes also promote photocleavage of plasmid pBR322 DNA and were screened for antimicrobial activity.

Keywords: Co(III) complexes; Polypyridyl ligand; DNA-binding; Photocleavage; Biological activity

1. Introduction

The interaction of transition metal complexes with DNA has received more attention [1–4] and many complexes have been synthesized. Useful applications of these complexes require that the complex bind to DNA through an intercalative mode with the ligand intercalating into adjacent base pairs of DNA. Varying the substitutive group or substituent position in the intercalative ligand creates interesting difference in space configuration and electron density distribution of transition metal complexes, resulting in differences in spectral properties and DNA-binding behaviors; this will be helpful in understanding the binding mechanism of transition metal complexes to DNA [5–7]. There have been intensive efforts to investigate factors that determine affinity and selectivity in binding of small molecules to DNA [8], because information about these factors would be invaluable in design of sequence-specific DNA-binding molecules for application in chemotherapy and in the development of tools for biotechnology [9]. Recently our group reported [10–12] DNA-binding and photocleavage studies of several mixed ligand complexes of ruthenium(II) and cobalt(III). In this article we

*Corresponding author. Email: ssnsirasani@yahoo.com

Journal of Coordination Chemistry
ISSN 0095-8972 print/ISSN 1029-0389 online
DOI: 10.1080/00958970903215081

report three Co(III) mixed polypyridyl complexes, $[Co(bpy)_2MHPIP]^{3+}$ (**1**), $[Co(dmb)_2MHPIP]^{3+}$ (**2**), and $[Co(phen)_2MHPIP]^{3+}$ (**3**), and the DNA-binding behavior from absorption and emission spectroscopy, DNA-melting techniques, viscosity measurements, and their abilities to induce cleavage of pBR322 DNA. The study also includes testing of the Co(III) complexes for antimicrobial activity.

2. Experimental

2.1. *Materials*

$CoCl_2 \cdot 6H_2O$, 1,10-phenanthroline monohydrate, and 2,2′-bipyridine were purchased from Merck (India). Calf-thymus-DNA (CT-DNA), tetrabutylammoniumchloride (TBACl), tetrabutylammoniumhexafluorophosphate ($TBAPF_6$), and 4,4′-dimethyl-2,2′-bipyridine were obtained from Sigma (St. Louis, MO, USA). Super coiled (CsCl purified) pBR322 DNA (Bangalore Genei, India) was used as received. All other common chemicals and solvents were procured from locally available sources; solvents were purified before use as per standard procedures [13]. Deionized, double distilled water was used for preparing various buffers. Solutions of DNA in Tris-HCl buffer (pH = 7.2), 50 mM NaCl gave a ratio of 1.8 : 1.9 UV absorbance at 260 and 280 nm, indicating the DNA was sufficiently free of protein [14]. The concentration of CT-DNA was determined spectrophotometrically using the molar absorption coefficient 6600 $M^{-1}\,cm^{-1}$ (260 nm) [15].

2.2. *Synthesis and characterization*

The compounds 1,10-phenanthroline-5,6-dione [16], $[Co(bpy)_2Cl_2]Cl$, $[Co(dmb)_2Cl_2]Cl$ [17], and $[Co(phen)_2Cl_2]Cl$ [18] were prepared according to literature procedures. Synthesis of ligands and their Co(III) complexes are shown in scheme 1.

2.2.1. Synthesis of MHPIP. MHPIP was prepared as per Steck and Day [19]. A solution of 1,10-phenanthroline-5,6-dione (0.260 g, 1.2 mmol), 3-methylsalysilaldehyde (0.245 g, 1.8 mmol), and ammonium acetate (1.9 g, 25 mmol) in 10 mL glacial acetic acid was refluxed for 2 h. The deep red solution obtained was cooled, diluted with water (25 cm^3), and neutralized with ammonia. Then the mixture was filtered, the precipitate was washed with H_2O and Me_2CO, and then dried (Yield: 80%). $C_{20}H_{14}N_4O$; Calcd (%); C, 73.61; H, 4.32; N, 17.17. Found (%): C, 73.40; H, 4.16; N, 17.38. ESI-MS (in DMSO), m/z; 327 (Calcd 326); IR (KBr): 1654 (C=N), 1504 (C=C) cm^{-1}; UV-Visible (CH_3OH), λ_{max}, nm ($\log \varepsilon$): 383(3.18), 341(2.77), 336(2.75), 288(2.81), 268(2.83), 246(2.77), 216(2.75). ^{1}H-NMR (DMSO-d_6, 25°C, δ ppm): 9.12 ppm (1H-4, s); 9.01 ppm (2H-1,d); 8.92 ppm (2H-3, d); 8.03 ppm (1H-7, s); 7.82 ppm (2H-2, m); 7.15 ppm (1H-5,d); 6.92 ppm (1H-6, d); 5.80 ppm (1H-9, NH, s); 2.30 ppm (3H-8, s); ^{13}C[^{1}H]-NMR (DMSO-d_6, δ ppm): 148, 146.5, 143, 134, 131, 130, 128, 126, 124, 123, 122, 116.5, 116, 115.5, 113, 110, and 21.5 ppm.

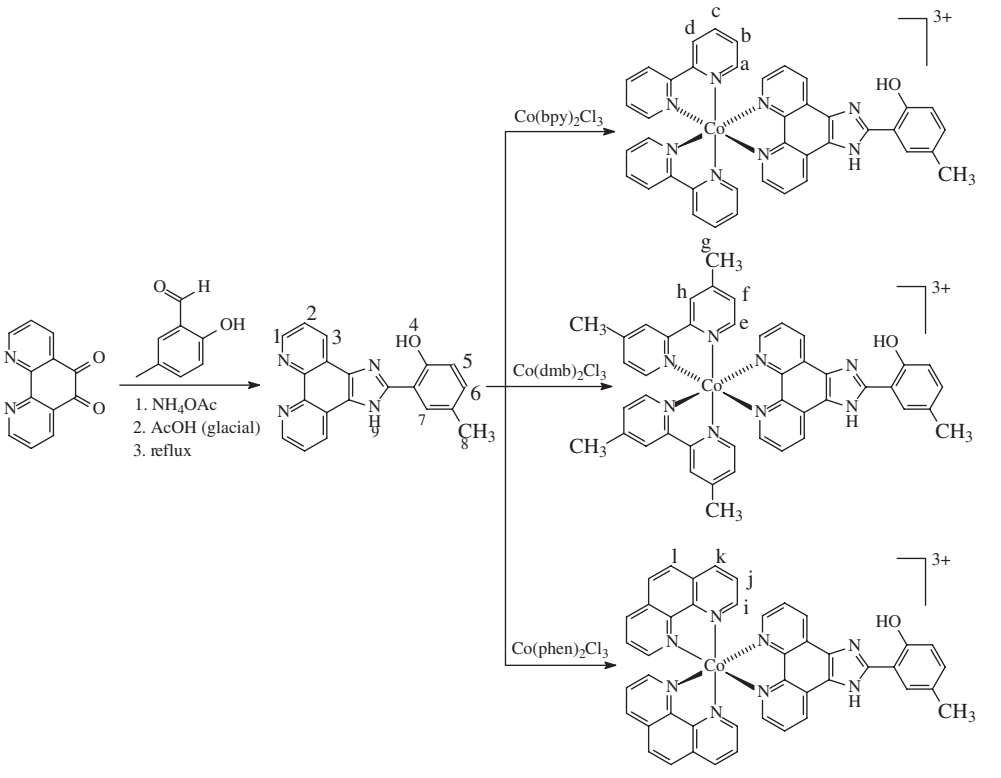

Scheme 1. Synthetic routes of ligand and Co(III) complexes.

2.2.2. Synthesis of $[Co(bpy)_2(MHPIP)](ClO_4)_3 \cdot 2H_2O$. A mixture of *cis*-$[Co(bpy)_2Cl_2]Cl \cdot 3H_2O$ (0.531 g, 1.0 mmol), MHPIP (0.489 g, 1.5 mmol) in EtOH (50 cm^3) was refluxed for 4 h to give a yellow solution. After filtration, the complex was precipitated by addition of a saturated ethanolic solution of $NaClO_4$. The complex was filtered and further dried under vacuum before recrystallization (Me_2CO–Et_2O). (Yield: 75%). $C_{40}H_{34}N_8Cl_3O_{15}Co$; Calcd (%): C, 46.57; H, 3.29; N, 10.86. Found (%): C, 46.21; H, 3.13; N, 11.13. LC-MS (in CH_3CN), *m*/*z*; 1032 (Calcd 1031). IR (KBr): 1466 (C=N), 1374 (C=C), 627 (Co–N (mhpip)), 476 (Co–N(bpy)) cm^{-1}: UV-Vis (CH_3OH), λ_{max}, nm ($\log \varepsilon$): 253(3.55), 258(3.54), 293(4.12), 331(3.67); ^{1}H-NMR (DMSO-d_6, 25°C, δ ppm): 9.02 ppm (6H-a and 1,d); 8.53 ppm (6H-c and 3,m); 7.91 ppm (1H-7,s); 7.80 ppm (6H-b and 2,m); 7.59 ppm (2H-5 and 6,d); 7.48 ppm (4H-d,d); 2.40 ppm (3H-8,s). ^{13}C [^{1}H]-NMR (DMSO-d_6, δ ppm, major peaks): 155, 152, 144, 137, 134, 129, and 21.8 ppm. Molar conductance of 335 Ω^{-1} cm^{-1} mol^{-1} indicates 1 : 3 electrolyte.

2.2.3. Synthesis of $[Co(dmb)_2(MHPIP)](ClO_4)_3 \cdot H_2O$. This complex was obtained by a procedure similar to that described above, *cis*-$[Co(dmb)_2Cl_2]Cl \cdot 3H_2O$ (0.587 g, 1.0 mmol) in place of *cis*-$[Co(bpy)_2Cl_2]Cl \cdot 3H_2O$. Yield: (65%). $C_{44}H_{40}N_8Cl_3O_{14}Co$; Calcd (%): C, 49.39; H, 3.74; N, 10.52. Found (%): C, 48.93; H, 3.27; N, 10.82. LC-MS

(in CH_3CN), m/z; 1070 (Calcd 1069). IR (KBr): 1438 (C=N), 1307 (C=C), 629 (Co–N(mhpip)), 485 (Co–N(dmb)) cm^{-1}; UV-Vis (CH_3OH), λ_{max}, nm ($\log \varepsilon$): 261(3.60), 271(3.58), 306(3.89), 329(3.28); ^{1}H-NMR (DMSO-d_6, 25°C, δ ppm): 9.03 ppm (2H-1,d); 8.96 ppm (4H-e,d); 8.49 ppm (2H-3,d); 7.88 ppm (1H-7,s); 7.72 ppm (6H-f and 2,m); 7.57 ppm (2H-5 and 6,d); 7.40 ppm (4H-h,s); 2.42 ppm (15H-g and 8,s). ^{13}C [^{1}H]-NMR (DMSO-d_6, δ ppm, major peaks): 156, 149.82, 143, 132, 128, and 21 ppm. Molar conductance of 341 $\Omega^{-1}\,cm^{-1}\,mol^{-1}$ indicates 1 : 3 electrolyte.

2.2.4. Synthesis of $[Co(phen)_2(MHPIP)](ClO_4)_3 \cdot 2H_2O$. This complex was obtained by a procedure similar to that described above, *cis*-$[Co(phen)_2Cl_2]Cl \cdot 3H_2O$ (0.578 g, 1.0 mmol) in place of *cis*-$[Co(bpy)_2Cl_2]Cl \cdot 3H_2O$. Yield: (60%). $C_{44}H_{34}N_8Cl_3O_{15}Co$; Calcd (%); C, 48.93; H, 3.15; N, 10.41%. Found (%): C, 49.15; H, 3.42; N, 10.27. IR (KBr): LC-MS (in CH_3CN), m/z; 1080 (Calcd 1079). 1424 (C=N), 1337 (C=C), 627 (Co–N(mhpip)), 456 (Co–N(bpy)) cm^{-1}. UV-Visible (CH_3OH), λ_{max}, nm ($\log \varepsilon$): 258(3.74), 276(3.93), 306(3.56), 328(3.38); ^{1}H-NMR (DMSO-d_6, 25°C, δ ppm): 9.30 ppm (2H-1,d); 9.25 ppm (4H-i,d); 8.80 ppm (5H-l and 7,s); 8.01 ppm (6H-k and 3,m); 7.80 ppm (6H-j and 2,m); 7.25 ppm (1H-5,d); 7.05 ppm (1H-6,d); 2.35 ppm (3H-8,s). ^{13}C [^{1}H]-NMR (DMSO-d_6, δ ppm, major peaks): 153.49, 146, 142, 132, 129, 128, and 21.4 ppm. Molar conductance of 343 $\Omega^{-1}\,cm^{-1}\,mol^{-1}$ indicates 1 : 3 electrolyte.

2.3. *Physical measurements*

UV-Visible spectra were recorded with an *Elico* Bio-spectro-photometer, model BL198. IR spectra were recorded in KBr discs on a Perkin-Elmer FT-IR-1605 spectrometer. ^{1}H-NMR spectra were measured on a Varian XL-300 MHz spectrometer using DMSO-d_6 as the solvent and TMS as an internal standard. Microanalyses (C, H, and N) were carried out on a Perkin-Elmer 240 elemental analyzer. Fluorescence spectra were recorded with a JASCO Model 7700 spectrofluorometer at the excitation wavelength. Viscosity experiments were carried on an Ostwald viscometer, immersed in a thermostatted water-bath at 30.0 ± 0.1°C. DNA samples approximately 200 base pairs in average length were prepared by sonication in order to minimize complexities arising from DNA flexibility [20]. Data were presented as $(\eta/\eta_0)^{1/3}$ *versus* concentration of [Co]/[DNA], where η is viscosity of DNA in the presence of complex and η_o is the viscosity of DNA alone. Viscosity values were calculated from the observed flow time of DNA-containing solutions ($t > 100$ s) corrected for the flow time of buffer alone (t_0), $\eta = t - t_0$ [21]. DNA-melting experiments were carried out by controlling the temperature of the sample cell with a Shimadzu circulating bath while monitoring the absorbance at 260 nm. For gel electrophoresis experiments, supercoiled pBR322 DNA (100 μM) was treated with Co(III) complexes in 50 mM Tris–HCl, 18 mM NaCl buffer pH 7.8, and the solutions were then irradiated at room temperature with a UV lamp (10 W). The samples were analyzed by electrophoresis for 2.5 h at 40 V on a 1% agarose gel in Tris-acetic acid–EDTA buffer, pH 7.2. The gels were stained with 1 μg mL^{-1} ethidium bromide and photographed under UV light.

The antimicrobial tests were performed by the standard disc diffusion method [22]. The complexes were screened for antifungal activity against *Aspergillus niger* and *Fusarium oxysporium* which were isolated from the infected parts of the host plants on M-test agar medium. The cultures of the fungi were purified by single-spore

isolation technique. A concentration of 1.5 mg mL^{-1} of each cobalt complex in DMSO was prepared for testing against spore germination of each fungus. Filter paper discs of 5 mm were prepared by using Whatman filter paper no. 1 (sterilized in an autoclave) saturated with 10 μL of the cobalt complex dissolved in DMSO or DMSO as negative control. The fungal culture plates were inoculated and incubated at 25 ± 2°C for 48 h. The plates were then observed and the diameters of the inhibition zones (in millimeters) were measured and tabulated. The results were also compared with a standard antifungal drug flucanazole at the same concentration.

The antibacterial activity of the complexes was studied against *Staphylococcus aureus* (MTCC 96) and *Escherichia coli* (MTCC 443). Each cobalt complex was dissolved in DMSO at 1 mg mL^{-1}. Paper discs of Whatman filter paper no. 1 were cut and sterilized in an autoclave. The paper discs were saturated with 10 μL of the cobalt complex dissolved in DMSO or DMSO as negative control and was placed aseptically in petridishes containing M-test agar media inoculated with *S. aureus* or *E. coli*. The petridishes were incubated at 37°C and the inhibition zones were recorded after 24 h. The experiments were repeated twice and average of the two was taken. The results were also compared with standard antibacterial drug streptomycin at the same concentration.

3. Results and discussion

3.1. *Characterization*

The ESI-MS spectra of MHPIP show a molecular ion peak at *m*/*z* 327, equivalent to its molecular weight (Calcd 326). ^{1}H-NMR spectra of the MHPIP gave a peak at 9.12 (singlet) corresponding to OH, a singlet at 2.30 corresponding to CH_3 protons, and a broad peak at 5.80 (singlet) corresponding to NH. Remaining signals belong to ring protons between 9.01 and 6.92 with proper multiplicity. The protons (C_1 and H) next to nitrogen appeared downfield as a doublet at 9.01. The ^{13}C-NMR of MHPIP gives a peak at 148 corresponding to carbon with OH (C_4), 146.5 corresponding to carbon next to nitrogen (C_1), and methyl carbon at 21.5. Other peaks are in the aromatic region. The LC-MS spectra of $[Co(bpy)_2(MHPIP)](ClO_4)_3 \cdot 2H_2O$ complex shows a molecular ion peak at *m*/*z* of 1032 which is equivalent to its molecular weight (Calcd 1031). The IR-spectra of $[Co(bpy)_2(MHPIP)](ClO_4)_3 \cdot 2H_2O$ have bands at 1466 (C=N) and 1374 (C=C), shifted to a lower frequency when compared to free ligand indicating complexation. New bands at 627 and 476 cm^{-1} in Co–N(mhpip) and Co–N(bpy) support complex formation. The ^{1}H-NMR spectra of $[Co(bpy)_2(MHPIP)](ClO_4)_3 \cdot 2H_2O$ show various protons of bpy and MHPIP shifted downfield upon complexation. In ^{13}C-NMR upon coordination of MHPIP to Co(III), the C_1 signal at 152 ppm, which is next to nitrogen, shifts downfield, the carbon attached to OH shifts downfield (155 (C_4)) and the methyl carbon resonates at 21.8. Peaks in the aromatic region also shift downfield. The LC-MS spectra of $[Co(dmb)_2(MHPIP)](ClO_4)_3 \cdot 2H_2O$ complex shows a molecular ion peak at *m*/*z* of 1070 which is equivalent to its molecular weight (Calcd 1069). In ^{1}H-NMR spectra peaks due to various protons of dmb and MHPIP ligands shift downfield upon complexation. In ^{13}C-NMR spectra C1 next to nitrogen shifts downfield by 7.5 ppm (C_1 and C_a), the carbon attached to OH shifts downfield to 156 (C_4), and methyl carbon resonates at 21. Aromatic peaks also shifted

downfield. LC-MS spectra of $[Co(phen)_2(MHPIP)](ClO_4)_3 \cdot 2H_2O$ show a molecular ion peak at m/z of 1080 (Calcd 1079); in ^{1}H-NMR spectra peaks due to various protons of phen and MHPIP ligands shift downfield upon complexation. The ^{13}C-NMR spectra show the carbon next to nitrogen shifted downfield to 146 (C_1 and C_a), the carbon attached to OH shifted downfield to 153.49 (C_4), and methyl carbon resonates at 21.4. Aromatic peaks also shift downfield.

3.2. *Electronic absorption*

Electronic spectroscopy in DNA-binding studies is one of the most useful techniques [23–25]. Complex binding with DNA through intercalation usually results in hypochromism and bathochromism. The extent of the hypochromism commonly parallels the intercalative binding strength. Electronic spectra of the complexes in the absence and presence of CT-DNA are illustrated in figure 1. The higher wavelength

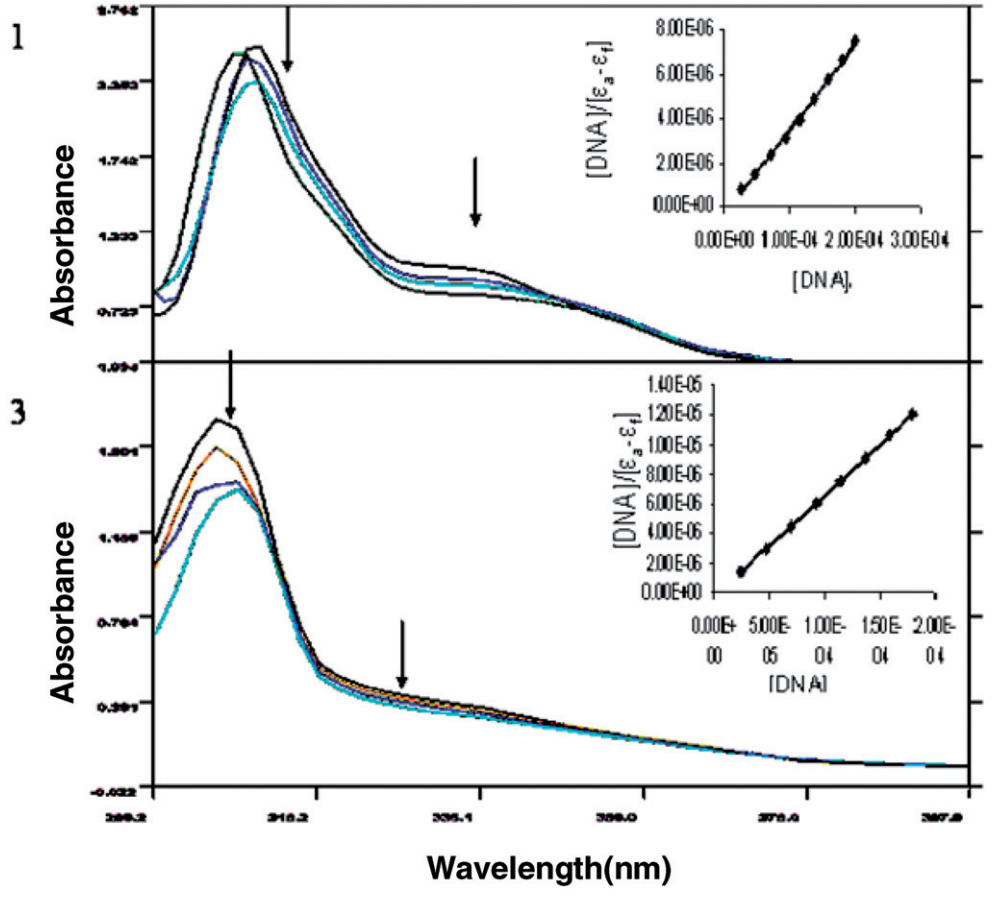

Figure 1. Absorption spectrum of $[Co(bpy)_2MHPIP]^{3+}$ (**1**) and $[Co(phen)_2MHPIP]^{3+}$ (**3**) in Tris-HCl buffer at 25°C in the presence of increasing amount of CT-DNA, [Co] = 10 μM, [DNA] = 0–120 μM. The arrows indicate the change in absorbance upon increasing the DNA concentration. Insert: Plot of $[DNA]/(\varepsilon_a - \varepsilon_f)$ *vs.* [DNA] for titration of the Co(III) complexes.

bands at λ_{max} 331 nm (for **1**), 329 nm (for **2**), and 328 nm (for **3**) are due to MLCT [26]. The higher energy bands at λ_{max} 258 nm (**1**), 261 nm (**2**), and 276 nm (**3**) are due to π–π^* transition of MHPIP. Addition of increasing quantities of CT-DNA results in decrease in peak intensities. Absorption spectra of $[Co(bpy)_2MHPIP]^{3+}$, $[Co(dmb)_2MHPIP]^{3+}$, and $[Co(phen)_2MHPIP]^{3+}$ in the absence and presence of CT-DNA (with subtraction of the DNA absorbance for the latter) at constant concentration of complexes are given in figure 1. Addition of increasing amounts of CT-DNA results in decrease in peak intensities in UV spectra for $[Co(bpy)_2MHPIP]^{3+}$, $[Co(dmb)_2MHPIP]^{3+}$, and $[Co(phen)_2MHPIP]^{3+}$, suggesting a mode of binding involving a stacking interaction between the complex and base pairs of DNA. To compare quantitatively the affinity of the three complexes toward DNA, the intrinsic binding constants K of the three complexes to CT-DNA were determined by monitoring the changes of absorbance at 331 nm (**1**), 329 nm (**2**), and 328 nm (**3**), with increasing concentration of DNA [26]. The intrinsic binding constants K of the three complexes with CT-DNA were determined according to following equation [27]:

$$[DNA]/(\varepsilon_a - \varepsilon_f) = [DNA]/(\varepsilon_b - \varepsilon_f) + 1/K(\varepsilon_b - \varepsilon_f)$$

where [DNA] is the concentration in the base pairs, the apparent absorption coefficients ε_a, ε_f, and ε_b correspond to $A_{obsd}/[Co]$, the extinction coefficient for the free cobalt complex, extinction coefficient of complex in the presence of DNA and the extinction coefficient for the cobalt complex in the fully bound form, respectively. In plots of $[DNA]/(\varepsilon_a - \varepsilon_f)$ *versus* [DNA], K is given by the ratio of slope to intercept. Intrinsic binding constants of $[Co(bpy)_2MHPIP]^{3+}$, $[Co(dmb)_2MHPIP]^{3+}$, and $[Co(phen)_2MHPIP]^{3+}$ were $2.2 \pm 0.2 \times 10^5$, $1.2 \pm 0.3 \times 10^5$, and $2.8 \pm 0.1 \times 10^5\ M^{-1}$, respectively. Addition of increasing amounts of CT-DNA results in hypochromism and moderate bathochromic shift in the UV spectra of the complexes in the order: $Co(phen)_2MHPIP]^{3+} > [Co(bpy)_2MHPIP]^{3+} > [Co(dmb)_2MHPIP]^{3+}$. These spectral characteristics suggest a stacking interaction between the complex and the base pairs of DNA.

The difference in binding strength of **1** and **2** could be attributed to different ancillary ligands. The four additional methyl groups in **2** exert some steric hindrance. Therefore, **1** is more deeply intercalated and more tightly bound to adjacent DNA base pairs than **2**. Similarly, the difference in binding strength of **1** and **3** is due to the difference in the ancillary ligands. On going from bpy to phen, the planar area and hydrophobicity increase leading to greater binding affinity for **3** than **1**. Zhang *et al.* [28, 29] studied binding of $[Co(phen)_2HPIP]^{3+}$ and $[Co(phen)_2HNOIP]^{3+}$ with CT-DNA, with $[Co(phen)_2HNOIP]^{3+}$ binding more weakly. In our studies we also observe that $[Co(phen)_2MHPIP]^{3+}$ binds weaker compared to $[Co(phen)_2HPIP]^{3+}$ with binding constant comparable to $[Co(phen)_2HNOIP]^{3+}$. The difference in these two complexes is NO_2 replaced with methyl.

3.3. *Fluorescence spectroscopic studies*

In the absence of DNA, **1**–**3** can emit luminescence in Tris buffer at ambient temperature, with maxima at ~560 nm. Upon addition of CT-DNA, the fluorescence emission intensities of **3**, **2**, and **1** increased by factors of 2.5, 1.75, and 2.2, respectively (Supplementary material), implying that the complexes encounter a hydrophobic

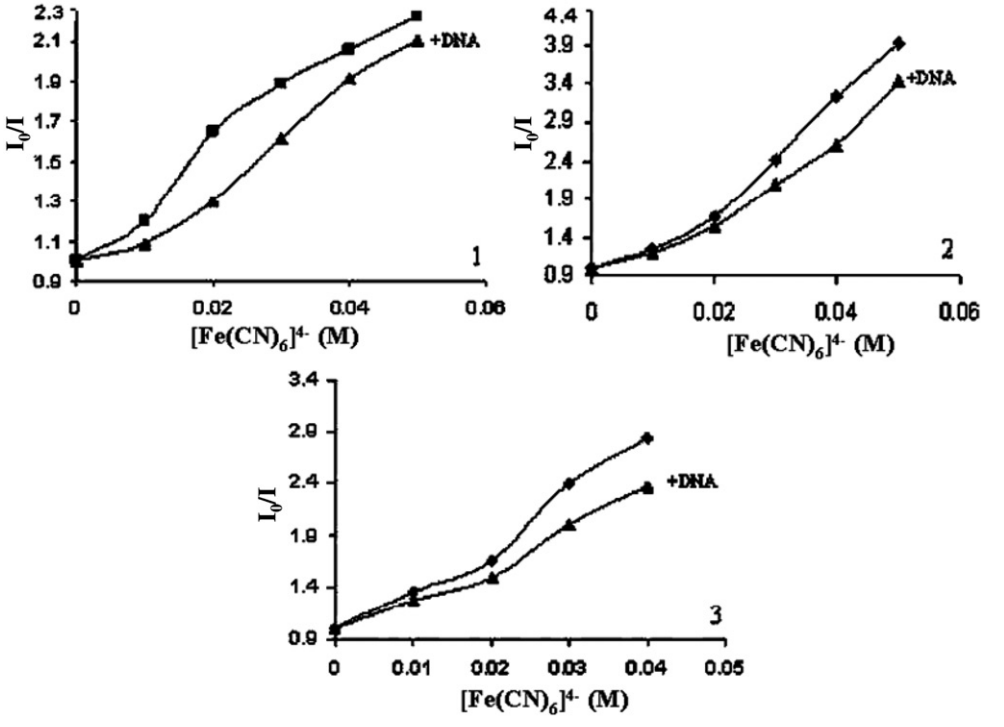

Figure 2. Emission quenching of Co(III) complexes **1**–**3** with $K_4[Fe(CN)_6]$ in the presence and absence of DNA. [Co] = 10 μM, [DNA]/[Co] = 40 : 1.

environment inside DNA. This restricts complex mobility leading to a decrease in vibrational modes of relaxation and hence increases the fluorescence intensity. The increase in fluorescence intensity supports the order of binding of complexes based on absorption studies. This is further supported by emission quenching experiments using $[Fe(CN)_6]^{4-}$, which permits distinguishing bound Co(III) species. Positively charged free complex ions should be readily quenched by $[Fe(CN)_6]^{4-}$. The complex bound to DNA can be protected from the quencher because the highly negative charges of $[Fe(CN)_6]^{4-}$ would be repelled by the negative DNA phosphate backbone, hindering quenching of the emission of the bound complex. The method essentially consists of titrating a given amount of DNA–metal complexes while increasing the concentration of $[Fe(CN)_6]^{4-}$ and measuring the change in fluorescence intensity. Ferro-cyanide quenching curves for these three complexes in the presence and absence of CT-DNA are shown in figure 2. The absorption and fluorescence studies indicate the binding of complexes and quenching studies also make clear that the order of binding of the complexes with DNA is $3 > 1 > 2$.

3.4. *Viscosity studies*

To further clarify the interaction between the complexes and DNA, viscosity measurements were carried out; since hydrodynamic measurements are sensitive to length increases (i.e. viscosity and sedimentation) these can be critical tests of the binding

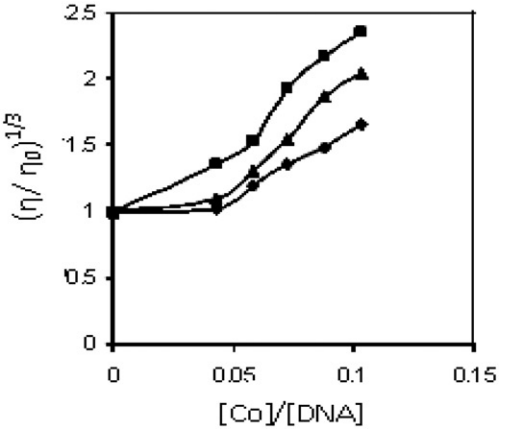

Figure 3. Effect of increasing amount of complexes $[Co(phen)_2MHPIP]^{3+}$ (■), $[Co(bpy)_2MHPIP]^{3+}$ (▲), and $[Co(dmb)_2MHPIP]^{3+}$ (◆) on relative viscosity of CT-DNA at 30.0 ± 0.1°C. The total concentration of DNA is 0.25 mM, [Co] = 10 μM.

Table 1. Results of absorption titration and thermal melting experiments.

			Absorption λ_{max} (nm)		
Complexes	T_m (°C)	Hypochromicity (%)	Free	Bound	Δλ
CT-DNA alone	60	–	–	–	–
$[Co(bpy)_2MHPIP]^{3+}$	64	11.5	258	266	8
$[Co(dmb)_2MHPIP]^{3+}$	62	8.9	261	266	5
$[Co(phen)_2MHPIP]^{3+}$	66	20.6	276	286	10

model in solution in the absence of crystallographic structural data [23, 30]. A classical intercalation model results in lengthening of the DNA helix, as base pairs are separated to accommodate the binding of metal complex, leading to an increase in DNA viscosity. Under appropriate conditions, intercalation of drugs like ethidium bromide (EtBr) causes a significant increase in the overall DNA length. On the other hand, partial and/or nonclassical intercalation of the ligand may bend (or kink) the DNA helix, resulting in the decrease in its effective length, and concomitantly, its viscosity. The effects of the three complexes on the viscosity of rod-like DNA are shown in figure 3. As the concentration of the complexes increases, the relative viscosity of DNA increases, as with the proven DNA intercalator $[Ru(phen)_2dppz]^{2+}$ [31], further suggesting that these Co(III) complexes show intercalative binding to CT-DNA. The small differences between **1** and **3** in the trend in viscosity are due to the ancillary ligands.

3.5. *DNA-melting studies*

Since DNA-melting experiments are useful in establishing the extent of intercalation [32], the three complexes ([Co] = 10 μM) were incubated with CT-DNA (100 μM), heated to 85°C from ambient temperature and the OD at 260 nm was monitored [33]. Binding of complexes leads to an increase in ΔT_m of DNA, in the order $[Co(phen)_2MHPIP]^{3+} > [Co(bpy)_2MHPIP]^{3+} > [Co(dmb)_2MHPIP]^{3+}$ (table 1).

3.6. *Photoactivated cleavage of pBR322 DNA*

Plasmid pBR322 DNA was subjected to gel electrophoresis after incubation with the cobalt(III) complexes and irradiation with 258, 261, and 276 nm for **1**, **2**, and **3**, respectively. In controls in which the complexes were absent (lane 1) as well as in DNA-complex adducts incubated in the dark (S1 Supplementary material) no photocleavage was noticeable. In contrast, with increasing concentration of the three complexes (lanes 2–5) and after irradiation, the amount of supercoiled form of pBR322 DNA diminishes gradually, whereas the nicked, slower moving, open circular form [34, 35] increases. Under comparable experimental conditions, all complexes exhibit effective photosensitized cleavage of DNA.

3.7. *Antimicrobial activity*

The antifungal activity data (table 2) indicate that the complexes show appreciable activity against *A. niger* and *F. oxysporium* at 1.5 mg mL^{-1} concentration. DMSO control has negligible activity compared to the metal complexes. The experimental results of the compounds were compared against DMSO as the control and are expressed as inhibition zone diameter (in millimeter) *versus* control. The complexes are more effective against *A. niger* than *F. oxysporium*. $[Co(phen)_2MHPIP]^{3+}$ shows the highest activity (22 mm) against *A. niger* at 1.5 mg mL^{-1} for the metal complexes. The same complex also shows the moderate activity (20 mm) against *F. oxysporium*. The same metal complex exhibited greater antifungal activity against *A. niger* compared to the standard drug flucanazole. The $[Co(bpy)_2MHPIP]^{3+}$ and $[Co(dmb)_2MHPIP]^{3+}$ complexes show less activity against these fungi than flucanazole.

The antibacterial activity data (table 3) indicate that the complexes have high activity against *S. aureus* and *E. coli* at 1 mg mL^{-1} concentration. DMSO control has negligible

Table 2. Antifungal activity of the cobalt complexes.

	Inhibition zone diameter (mm) of fungal species	
Complex	*A. niger*	*F. oxysporium*
$[Co(bpy)_2MHPIP]^{3+}$ (**1**)	10.0 ± 0.2	12.0 ± 0.4
$[Co(dmb)_2MHPIP]^{3+}$ (**2**)	12.0 ± 0.1	11.0 ± 0.2
$[Co(phen)_2MHPIP]^{3+}$ (**3**)	22.0 ± 0.3	20.0 ± 0.1
Flucanazole (standard)	15–18	15–18

Table 3. Antibacterial activity of the cobalt complexes.

	Inhibition zone diameter (mm) of bacterial species	
Complex	*S. aureus*	*E. coli*
$[Co(bpy)_2MHPIP]^{3+}$ (**1**)	11.0 ± 0.3	10.0 ± 0.1
$[Co(dmb)_2MHPIP]^{3+}$ (**2**)	10.0 ± 0.4	9.0 ± 0.4
$[Co(phen)_2MHPIP]^{3+}$ (**3**)	19.0 ± 0.1	18.0 ± 0.2
Streptomycin (standard)	13–17	13–17

activity compared to the metal complexes. The experimental results are expressed as inhibition zone diameter (in millimeter) *versus* control. The complexes are more effective against *S. aureus* than *E. coli*. $[Co(phen)_2MHPIP]^{3+}$again shows the highest activity (19 mm) against *S. aureus* at $1\,mg\,mL^{-1}$ among all the metal complexes. The same complex also shows activity of 18 mm inhibition against *E. coli*. The same metal complex exhibits greater antibacterial activity against *S. aureus* than the standard drug streptomycin. $[Co(bpy)_2MHPIP]^{3+}$ and $[Co(dmb)_2MHPIP]^{3+}$ show less activity against these bacteria than streptomycin. The three metal complexes possess antifungal and antibacterial activity. Earlier studies have also shown results similar to this study [36, 37].

4. Conclusion

The three Co(III) complexes, $[Co(bpy)_2MHPIP]^{3+}$, $[Co(dmb)_2MHPIP]^{3+}$, and $[Co(phen)_2MHPIP]^{3+}$, have been synthesized and characterized. Spectroscopic studies and viscosity experiments indicated that the three complexes intercalate into DNA base pairs via the MHPIP ligand and the difference in the binding constant is due to the difference in ancillary ligands. Comparison of our results with literature reveals that the binding constant largely depends on the intercalating ligand and very little on ancillary ligands and metal ion. As the planarity of the intercalating ligand increases binding constant increases and asymmetry of the ligand makes it difficult to intercalate and hence binding constant decreases. Many applications [38, 39] require that the complex interact with DNA through intercalation. The aim of the present study is to know how best the complex is interacted with DNA through intercalation. Absorption, thermal melting and viscosity studies helped in establishing the intercalative binding. When irradiated, the Co(III) complexes are efficient photocleavers of plasmid pBR322 DNA. Complex **3** shows activity slightly more than standard drugs against bacterial species.

Acknowledgement

The financial support from UGC (New Delhi) is gratefully acknowledged.

References

[1] K.E. Erkkila, D.T. Odom, J.K. Barton. *Chem. Rev.*, **99**, 2777 (1999).
[2] M. Demeunynck, C. Bailly, W.D. Wilson (Eds), *DNA and RNA Binders*: *From Small Molecules to Drugs*, Wiley-VCH, Weinheim (2003).
[3] M. Gielen, E.R.T. Tickink (Eds), *Metallotherapeutic Drugs and Metal-Based Diagnostic Agents. The Use of Metals in Medicine*, John Wiley & Sons, New York, NY, USA (2005).
[4] B. Peng, H. Chao, B. Sun, H. Li, F. Gao, L.-N. Ji. *J. Inorg. Biochem.*, **101**, 404 (2007).
[5] C. Metcalfe, J.A. Thomas. *Chem. Soc. Rev.*, **32**, 215 (2003).
[6] I. Ortmans, C. Moucheron, A. Kirsch-De Mesmaeker. *Coord. Chem. Rev.*, **168**, 233 (1998).
[7] H. Choa, L.N. Ji. *Bioinorg. Chem. Appl.*, **3**, 15 (2005).
[8] J.K. Barton. *Science*, **223**, 727 (1986).
[9] A.M. Pyle, J.P. Rehman, R. Mesnoyrer, C.V. Kumar, N.J. Turro, J.K. Barton. *J. Am. Chem. Soc.*, **111**, 3051 (1989).

[10] P. Nagababu, S. Satyanarayana. *Polyhedron*, **26**, 1686 (2007).
[11] P. Nagababu, D. Aravind Kumar, K.L. Reddy, K. Ashwini Kumar, Md.B. Mustafa, M. Shilpa, S. Satyanarayana. *Metal-Based Drugs* (2008), doi:10.1155/2008/275084, pp. 1–8.
[12] P. Pallavi, P. Nagababu, S. Satyanarayana. *Helv. Chim. Acta*, **90**, 627 (2007).
[13] D.D. Perrin, W.L.F. Annarego, D.R. Perrin. *Purification of Laboratory Chemicals*, 2nd Edn, Pergamon Press, New York (1980).
[14] J. Marmur. *J. Mol. Biol.*, **3**, 208 (1961).
[15] M.E. Reichmann, S.A. Rice, C.A. Thomas, P. Doty. *J. Am. Chem. Soc.*, **76**, 3047 (1954).
[16] M. Yamada, Y. Tanaka, Y. Yoshimoto, S. Kuroda, I. Shimo. *Bull. Chem. Soc. Jpn.*, **65**, 1006 (1992).
[17] A.A. Vleek. *Inorg. Chem.*, **6**, 1425 (1967).
[18] A.V. Ablore. *Russ. J. Inorg. Chem.*, **6**, 157 (1961).
[19] E.A. Steck, A.R. Day. *J. Am. Chem. Soc.*, **65**, 452 (1943).
[20] J.B. Chaires, N. Dattaguptha, D.M. Crother. *Biochemistry*, **21**, 3933 (1982).
[21] S. Satyanarayana, J.C. Dabrowiak, J.B. Chaires. *Biochemistry*, **32**, 2573 (1993).
[22] W.L. Drew, A.L. Barry, R. O'Toole, J.C. Sherris. *Appl. Microbiol (American Society for Microbiology)*, **24**, 240 (1972).
[23] J.K. Barton, A.L. Raphael. *J. Am. Chem. Soc.*, **106**, 2172 (1984).
[24] T.M. Kelly, A.B. Tossi, D.J. Mc Connell, T.C. Stekas. *Nucleic Acids Res.*, **106**, 2172 (1984).
[25] S.A. Tysoe, R.J. Morgan, A.D. Baker, T.C. Strekas. *J. Phys. Chem.*, **97**, 1707 (1993).
[26] H.-L. Chen, P. Yang. *Chin. J. Chem.*, **20**, 1529 (2002).
[27] A. Wolfe, G.H. Shimer, T. Mechan. *Biochemistry*, **26**, 6392 (1984).
[28] Q.L. Zhang, J.G. Liu, H. Xu, H. Li, J.Z. Liu, H. Zhou, L.H. Qu, L.N. Ji. *Polyhedron*, **20**, 3049 (2001).
[29] Q.L. Zhang, J.G. Liu, J.Z. Liu, H. Li, Y. Yang, H. Xu, H. Chao, L.N. Ji. *Inorg. Chim. Acta*, **339**, 34 (2002).
[30] S. Satyanarayana, J.C. Dabrowiak, J.B. Chaires. *Biochemistry*, **31**, 9319 (1992).
[31] I. Haq, P. Lincoln, D. Suh, B. Norden, B.Z. Chowdhry, J.B. Chaires. *J. Am. Chem. Soc.*, **117**, 4788 (1995).
[32] T.M. Kelly, A.B. Tossi, D.J. Mc Connell, C. Ohuigin. *Nucleic Acids Res.*, **13**, 6017 (1985).
[33] E. Tselepi-Kalouli, N. Katsaros. *J. Inorg. Biochem.*, **37**, 271 (1989).
[34] R.P. Hertzberg, P.B. Dervan. *J. Am. Chem. Soc.*, **104**, 313 (1982).
[35] D.S. Sigman, D.R. Graham, L.E. Marshall, K.A. Reich. *J. Am. Chem. Soc.*, **102**, 5419 (1980).
[36] M.S. Islam, M.B. Hossain, M.Y. Reza. *J. Med. Sci.*, **3**, 289 (2003).
[37] F.M. Morad, M.M.E. Lajaily, S.B. Gweirif. *J. Sci. Appl.*, **1**, 72 (2007).
[38] Y. Liu, Y.-J. Liu, J.-H. Yao, W.-J. Mei, F. Haiwu. *J. Coord. Chem.*, **62**, 1701 (2009).
[39] Y.-J. Liu, J.-F. He, J.-H. Yao, W.-J. Mei, F. Haiwu, L.-X. He. *J. Coord. Chem.*, **62**, 665 (2009).